Effects of the transition zone on the surface tension of Ar near the triple point

Chia C. Shih and Yea H. Uang

Department of Physics and Astronomy, University of Tennessee, Knoxville, Tennessee 37916

(Received 13 August 1976)

The effect of the transition zone on the surface tension of Ar near the triple point is reexamined. The surface tension is calculated from the Kirkwood-Buff formula for the cases of a linear density profile and also a cubic profile and the formulas differ from those previously obtained by Fitts. The realistic Barker-Fisher-Watts potential is used and the radial distribution function in the bulk liquid is taken from experiment. Several approximate representations of the distribution function in the transition zone are used. The results indicate that the surface tension is a slowly varying function of the thickness of the transition zone, and that Fowler's step-function profile does not introduce substantial error. When this value is combined with the three-body nonadditivity contribution, the total tension is significantly smaller than the experimental value.

I. INTRODUCTION

Recently Present and Shih[1] extended the Kirk-wood-Buff (KB) molecular theory[2] of surface tension to include the three-body interactions. Assuming a step-function profile (Fowler),[3] a superposition triplet-correlation function (Kirkwood), and a triple-dipole interaction (Axilrod-Teller),[4] the nonadditivity correction γ_3 to the surface tension was expressed as an integral containing the radial distribution function $g(r)$ of the liquid as the weighting factor. Taking the neutron diffraction data of Yarnell *et al.*[5] for liquid Ar at 85°K to represent $g(r)$, the resultant γ_3 for Ar at 85°K was estimated to be −4.5 dyn/cm. This value is in good agreement with the value of −4.0 dyn/cm at 84°K calculated by Lee, Barker, and Pound[6] using a completely different Barker-Henderson (BH) perturbation theory.[7]

However, difficulties arise when the nonadditivity correction is combined with γ_2, the surface tension computed in the Kirkwood-Buff-Fowler (KBF) approximation from realistic pair potentials for Ar using the same $g(r)$ data.[8] The total surface tension $(\gamma_2 + \gamma_3)$ gave 9.2 dyn/cm for the Baker-Fisher-Watts potential[9] and 10.5 dyn/cm for the MSV-III potential of Parson, Siska, and Lee[10] as compared to the experimental surface tension of 13.1 dyn/cm. This difficulty is nevertheless absent in the calculations of Lee, Barker, and Pound.[6] Their estimation of the two-body contribution was 16.87 dyn/cm based on the Baker-Fisher-Watts potential and the BH perturbation theory, and 16.18 dyn/cm based on a Monte Carlo model using a Lennard-Jones 12-6 potential. The total surface tension of 12.88 dyn/cm at 84°K based on the BH perturbation theory is much closer to the experimental value of 13.45 dyn/cm than that of the KB theory. A more recent Monte Carlo calculation by Miyazaki, Barker, and Pound[11] based on a direct evaluation of free energy

leads to a larger value of 18.3 dyn/cm for γ_2. And the Monte Carlo calculation by Chapela, Savilla, and Rowlinson[12] leads to an even larger value of γ_2.[13]

Both the BH perturbation theory and the Monte Carlo method possess a smooth transition zone between the liquid and vapor. It is, therefore, desirable to extend the KBF calculation to a more realistic profile for a possible conciliation of the difference between the estimations of γ_2. Calculations along this direction already exist. Using the incorrect extensions of the KB formula for the smooth profile by Fitts,[14] Freeman and McDonald calculated the dependence of the surface tension on the transition zone with a linear, a cubic, and an exponential profile.[15] From a Monte Carlo numerical integration with a Lennard-Jones 12-6 potential, their resultant surface tension gave 13.7 dyn/cm at zero width (Fowler step-function approximation).[3] For the linear and the cubic profile, this value remained constant when the total width of the transition zone d was less than d_0, the distance of closest approach of the molecules in the liquid [$g(d_0) = 0$]. It then rose rapidly to a maximum of 16−17 dyn/cm for d in the region between d_0 and $2d_0$. This feature did not exist for the exponential profile. By contrast, the surface tension mostly decreased slowly as d increased.

In the following we shall calculate the surface tension γ_2 for several liquid density profiles. In order to probe the structures of the transition zone, we shall also introduce several phenomenological radial distribution functions in this region. The latter extension increases considerably the algebra in calculating the traditional superficial densities in the KB formulations. It is preferable to develop a shorter alternative algebraic procedure bypassing the Gibbs dividing surface and the superficial densities. Our resultant formulas include the terms that Fitts[14] has obtained but there

are additional terms that he has omitted. As a consequence, the dependence of γ_2 on the width of the transition zone is also different from that of Freeman and McDonald.[15]

II. EXTENSIONS OF KIRKWOOD-BUFF-FOWLER FORMULA

Starting from the Kirkwood-Buff formula[2] for the two-body contribution to the surface tension

$$\gamma_2 = \frac{1}{2} \int_{-\infty}^{\infty} dz_1 \rho(z_1) \int d\tau_{12} \rho(z_2) \frac{x_{12}^2 - z_{12}^2}{r_{12}}$$
$$\times \frac{du(r_{12})}{dr_{12}} g^{(2)}(z_1, z_2, r_{12}) , \tag{1}$$

we shall take the vapor-phase density occupying z

≤ 0 to be effectively zero. The density of the liquid Ar is taken to be a constant ρ_l for $z \ge d$. In between the two layers the liquid density profile is taken as either a linear profile

$$\rho(z)/\rho_l = z/d, \quad 0 \le z \le d \tag{2a}$$

or a cubic profile

$$\rho(z)/\rho_l = 3z^2/d^2 - 2z^3/d^3, \quad 0 \le z \le d . \tag{2b}$$

When both z_1 and z_2 are in the bulk liquid, there is no ambiguity for the radial distribution function, $g_l(r_{12})$, which we take from the neutron diffraction data of Yarnell et al.[5] When z_1 and/or z_2 are in the transition zone, the $g^{(2)}$ is, however, uncertain. Because of possible mixing of the liquid and the vapor, we shall therefore parametrize it in the following ways:

no-mixing,

$$g^{(2)}(z_1, z_2, r_{12}) = g_l(r_{12}) , \tag{3a}$$

linear-mixing,[16]

$$g^{(2)}(z_1, z_2, r_{12}) = \begin{cases} g_l(r_{12}) + [1 - (z_1 + z_2)/2d][g_v(r_{12}) - g_l(r_{12})], z_1, z_2 < d \\ g_l(r_{12}) + (1 - z_1/d)[g_v(r_{12}) - g_l(r_{12})], z_1 \le d \le z_2 \end{cases} \tag{3b}$$

quadratic-mixing,

$$g^{(2)}(z_1, z_2, r_{12}) = \begin{cases} g_l(r_{12}) + (1 - z_1 z_2/d^2)[g_v(r_{12}) - g_l(r_{12})], z_1, z_2 < d \\ g_l(r_{12}) + (1 - z_1/d)[g_v(r_{12}) - g_l(r_{12})], z_1 \le d \le z_2 \end{cases} \tag{3c}$$

where $g_v(r_{12}) = \exp[-u(r_{12})/kT]$ is the radial distribution function of vapor Ar. We shall outline briefly the algebraic procedure and leave the details to the Appendix, for the interested readers. Instead of introducing a Gibbs surface, we shall first rewrite Eq. (1) in terms of the spherical coordinates of $\vec{r}_{12}$ as follows:

$$\gamma_2 = \frac{\pi}{2} \int_0^{\infty} dz_1 \rho(z_1) \int_{\max(0, z_1 - d)}^{\infty} dr_{12} r_{12}^3 u'(r_{12}) \int_{\max(-1, -z_1/r_{12})}^{1} d\omega (1 - 3\omega^2) \rho(z_2) g^{(2)}(z_1, z_2, r_{12}) , \tag{4}$$

where $\omega = z_{12}/r_{12}$. Here a spherical region $r_{12} \le \max(0, z_1 - d)$ is deleted because of the symmetry between x_{12} and z_{12}. Interchanging r_{12} and z_1 and replacing ω by z_2 we get

$$\gamma_2 = \frac{\pi}{2} \int_0^{\infty} dr_{12} u'(r_{12}) \int_0^{r_{12} + d} dz_1 \rho(z_1) \int_{\max(0, z_1 - r_{12})}^{z_1 + r_{12}} dz_2 \rho(z_2)[r_{12}^2 - 3(z_1 - z_2)^2] g^{(2)}(z_1, z_2, r_{12}) . \tag{5}$$

The explicit symmetry between z_1 and z_2 can be restored if we calculate the difference between γ_2 and γ_F (Fowler) associated with the step-function profile $\rho(z) = \rho_l$, $z \ge 0$, with

$$\gamma_F = \frac{\pi \rho_l^2}{8} \int_0^{\infty} dr_{12} r_{12}^4 u'(r_{12}) g_l(r_{12}) . \tag{6}$$

The final expression which can be readily evaluated is then

$$\gamma_2 - \gamma_F = \pi \int_0^{\infty} dr_{12} u'(r_{12}) \int_0^d dz_1 \rho(z_1) \int_{z_1}^{z_1 + r_{12}} dz_2 \rho(z_2) g^{(2)}(z_1, z_2, r_{12})[r_{12}^2 - 3(z_1 - z_2)^2] . \tag{7}$$

In this equation the integration over z_1 and z_2 can be carried out explicitly. We shall omit all the lengthy algebra and simply state the resultant formula:

$$\gamma_2 - \gamma_F = \frac{\pi \rho_l^2 d^4}{16} \int_0^{\infty} dr u'(r)\{g_l(r)\Delta_1(2r/d) + [g_v(r) - g_l(r)]\Delta_2(2r/d)\} . \tag{8}$$

For linear profile and no mixing,

$$\Delta_1(x) = (-\tfrac{1}{8} + \tfrac{1}{15}x - \tfrac{1}{96}x^2)x^4[1 - \Theta(\tfrac{1}{2}x)] + (\tfrac{2}{15} - \tfrac{1}{6}x^2)\Theta(\tfrac{1}{2}x) , \tag{8a}$$

where

$$\Theta(x) = \begin{cases} 0, & x < 1 \\ 1, & x \geq 1 . \end{cases}$$

For linear profile and linear mixing we need in addition to (8a), the function $\Delta_2(x)$

$$\Delta_2(x) = (-\tfrac{1}{30} + \tfrac{1}{96}x)x^5[1 - \Theta(\tfrac{1}{2}x)] + (\tfrac{4}{15} - \tfrac{1}{6}x^2)\Theta(\tfrac{1}{2}x) . \tag{8b}$$

For linear profile and quadratic mixing we need in addition to (8a), a different $\Delta_2(x)$,

$$\Delta_2(x) = (-\tfrac{1}{45} + \tfrac{1}{96}x - \tfrac{1}{2304}x^3)x^5[1 - \Theta(\tfrac{1}{2}x)] + (\tfrac{1}{15} - \tfrac{1}{18}x^2)\Theta(\tfrac{1}{2}x) . \tag{8c}$$

For cubic profile and no mixing, we need instead

$$\Delta_1(x) = (-\tfrac{1}{8} + \tfrac{2}{25}x - \tfrac{1}{70}x^3 + \tfrac{1}{256}x^4 - \tfrac{1}{12800}x^6)x^4[1 - \Theta(\tfrac{1}{2}x)] + (\tfrac{9}{175} - \tfrac{1}{10}x^2)\Theta(\tfrac{1}{2}x) . \tag{8d}$$

For cubic profile and linear mixing, we need in addition to (8d), the function $\Delta_2(x)$,

$$\Delta_2(x) = (-\tfrac{2}{75} + \tfrac{1}{140}x^2 - \tfrac{1}{768}x^3 - \tfrac{1}{25600}x^5)x^5[1 - \Theta(\tfrac{1}{2}x)] + (\tfrac{27}{175} - \tfrac{7}{60}x^2)\Theta(\tfrac{1}{2}x) . \tag{8e}$$

And for cubic profile and quadratic mixing, we need in addition to (8d), a different $\Delta_2(x)$,

$$\Delta_2(x) = (-\tfrac{1}{105} + \tfrac{1}{192}x + \tfrac{1}{700}x^2 - \tfrac{1}{768}x^3 + \tfrac{1}{10240}x^5 - \tfrac{1}{268800}x^7)x^5[1 - \Theta(\tfrac{1}{2}x)] + (\tfrac{1}{105} - \tfrac{7}{600}x^2)\Theta(\tfrac{1}{2}x) . \tag{8f}$$

Note that Eqs. (8a) and (8d) are different from those of Refs. 11 and 12. There the $r_{12} < d$ ($x \leq 2$) terms are the same, but the $r_2 > d$ ($x > 2$) terms are absent. Whenever d is less than d_0, the radial distribution function suppresses the $r_{12} < d$ term completely, leaving the other term as the sole contribution to the surface tension. A careful re-examination of the situation corresponding to the

TABLE I. Dependence of surface tension of Ar γ_2 (dyn/cm) at 85 °K[a] on the transition-zone width d [Baker-Fisher-Watts potential (Ref. 9)].

Width d(Å)	Linear profile			Cubic profile		
	No mixing[b]	Linear mixing[c]	Quadratic mixing[d]	No mixing[e]	Linear mixing[f]	Quadratic mixing[g]
0	13.70	13.70	13.70	13.70	13.70	13.70
0.5	13.71	13.67	13.70	13.71	13.68	13.70
1.0	13.74	13.59	13.69	13.72	13.62	13.71
1.5	13.77	13.44	13.66	13.75	13.51	13.72
2.0	13.81	13.22	13.61	13.78	13.36	13.73
2.5	13.83	12.93	13.53	13.80	13.17	13.74
3.0	13.82	12.55	13.39	13.82	12.92	13.73
3.5	13.74	12.07	13.17	13.82	12.63	13.70
4.0	13.58	11.50	12.86	13.79	12.28	13.63
4.5	13.34	10.93	12.46	13.72	11.90	13.52
5.0	13.05	10.41	12.02	13.60	11.54	13.37
5.5	12.71	9.96	11.59	13.44	11.21	13.17
6.0	12.35	9.56	11.15	13.25	10.91	12.94
6.5	11.99	9.20	10.74	13.03	10.63	12.69
7.0	11.63	8.86	10.34	12.79	10.37	12.43

[a] The bulk density of Ar is taken to be 0.021 25 atoms/Å^3.
[b] Equation (8a).
[c] Equations (8a) and (8b).
[d] Equations (8a) and (8c).
[e] Equation (8d).
[f] Equations (8d) and (8e).
[g] Equations (8d) and (8f).

TABLE II. Dependence of surface tension of Ar γ_2 (dyn/cm) at 85 °K[a] on the transition-zone width d [MSV-III potential (Ref. 10)].

| Width d(Å) | Linear profile | | | Cubic profile | | |
	No mixing[b]	Linear mixing[c]	Quadratic mixing[d]	No mixing[e]	Linear mixing[f]	Quadratic mixing[g]
0	14.99	14.99	14.99	14.99	14.99	14.99
0.5	14.99	14.95	14.98	14.99	14.96	14.99
1.0	14.99	14.82	14.94	14.99	14.87	14.98
1.5	14.99	14.62	14.86	14.99	14.73	14.96
2.0	14.97	14.32	14.75	14.98	14.53	14.94
2.5	14.92	13.94	14.59	14.97	14.27	14.90
3.0	14.84	13.47	14.37	14.94	13.96	14.84
3.5	14.69	12.90	14.07	14.88	13.60	14.75
4.0	14.47	12.26	13.69	14.80	13.19	14.63
4.5	14.17	11.64	13.23	14.68	12.76	14.46
5.0	13.82	11.08	12.75	14.51	12.35	14.26
5.5	13.45	10.59	12.27	14.31	11.98	14.02
6.0	13.05	10.17	11.80	14.07	11.64	13.75
6.5	12.66	9.78	11.35	13.81	11.33	13.46
7.0	12.27	9.42	10.93	13.54	11.04	13.16

[a] The bulk density of Ar is taken to be 0.021 25 atoms/Å^3.
[b] Equation (8a).
[c] Equations (8a) and (8b).
[d] Equations (8a) and (8c).
[e] Equation (8d).
[f] Equations (8d) and (8e).
[g] Equations (8d) and (8f).

linear and cubic profile using the alternative method of superficial densities leads to the same formula for Eq. (8a) and Eq. (8d).

III. NUMERICAL RESULTS AND DISCUSSIONS

The results of the numerical integrations of the above expressions using the Baker-Fisher-Watts potential for $u(r)$ and the Yarnell data for $g(r)$ are tabulated in Tables I and II. Note that for $d < d_0$, the surface tension generally varies slowly starting from the value 13.7 dyn/cm for Barker's potential and 15.0 dyn/cm for the MSV-III potential. Since there are some indications that d is close to d_0 for Ar near the triple point,[16] the Fowler step-function profile does not lead to severe error. For large d, the surface tension becomes substantially smaller. This behavior is consistent with that of the exponential profile in Ref. 14 using a Lennard-Jones 12-6 potential. None of the behavior shows any dramatic increase as a function of d. The

surface tension γ_2 is in all cases insensitive to the width of the transition zone. However, γ_2 is sensitive to the repulsive region of the intermolecular potential (Table III).

Since the surface tension γ_2 estimated by the BH theory and the Monte Carlo method are 16.87 and 16.18 dyn/cm, respectively, at 84 °K the differences between the different estimates of γ_2 are not removed.[13] According to the KBF formulation, the total value of the surface tension $\gamma_2 + \gamma_3$ is also much smaller than the value from BH perturbation theory. Extension of the KBF formula to include a transition zone only reduces further its value. This disagreement could be due to the approximate nature of the radial distribution function used in the transition zone or to the BH values of $g(r)$ differing from the Yarnell data. By using the phenomenological Yarnell data in the KBF formula, many-body interactions are implicitly included. As for the Monte Carlo calculation using Lennard-Jones 12-6 potentials, although the Lennard-Jones

TABLE III. Contributions of surface tension of Ar γ_2 (dyn/cm) at 85 °K[a] from the repulsive and attractive regions of intermolecular potentials with step-function density profile.

	γ_2 (repulsive)	γ_2 (attractive)	Total
Baker-Fisher-Watts	−12.02	25.72	13.70
MSV-III	−10.73	25.72	14.99

[a] The bulk density of Ar is taken to be 0.021 25 atoms/Å^3.
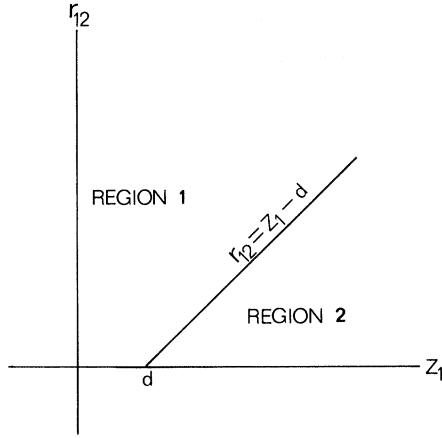
FIG. 1. Regions of integration. Particles 1 and 2 are all in the bulk liquid phase for region 2.

12-6 potential seems to mock up the many-body effects to $g(r)$ in the bulk liquid, it does not follow that it will do so near the surface of the liquid. Another source of difference may be due to a difference in the effective value of d_0. Since the contribution to γ_2 from the repulsive region of the intermolecular potential is negative (Table III) a larger value of d_0 in the KBF formula would lead to a larger value of γ_2.

The difference between the experimental value of the surface tension and the theoretical value from the KB theory may not be due to an underestimation in γ_2. It is possible that the use of the triple-dipole interactions overestimated the three-body
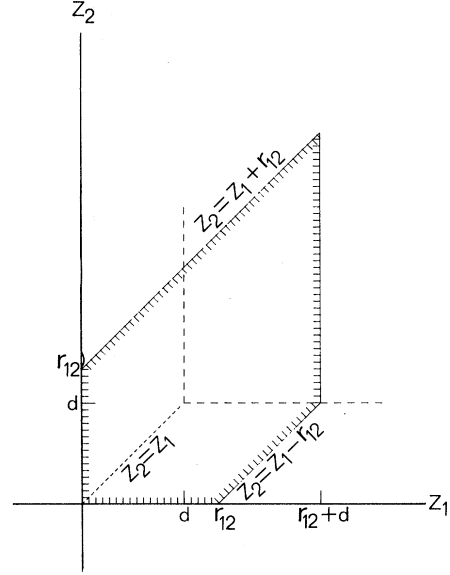
FIG. 2. Regions of integration in variable z_1 and z_2 with a given $r_{12} > d$. (For the case of $r_{12} < d$, the intersection of $z_2 = z_1 + r_{12}$ line to the z_2 axis would be lower then the $z_2 = d$ point. The shape of the regions is otherwise the same as the one before.)

nonadditivity correction (γ_3) or else n-body interactions with $n \geqslant 4$ are also important.

APPENDIX

Starting from Eq. (1), with $z_1, z_2 \geqslant 0$

$$\gamma_2 = \frac{1}{2} \int_0^\infty dz_1 \rho(z_1) \int_{-z_1}^\infty dz_{12} \int_{-\infty}^\infty dx_{12} \int_{-\infty}^\infty dy_{12} \frac{x_{12}^2 - z_{12}^2}{r_{12}} \rho(z_2) \frac{du(r_{12})}{dr_{12}} g^{(2)}(z_1, z_2, r_{12})$$

$$= \frac{1}{2} \int_0^\infty dz_1 \rho(z_1) \int dr_{12} r_{12}^3 u'(r_{12}) \int d\theta_{12} \sin\theta_{12} \rho(z_2) g^{(2)}(z_1, z_2, r_{12}) \int d\phi_{12}(\sin^2\theta_{12}\cos^2\phi_{12} - \cos^2\theta_{12}),$$

$$\tag{A1}$$

where $z_2 = z_1 + r_{12}\cos\theta_{12}$.

The region of integration can be split into regions 1 and 2 (Fig. 1),

$$\gamma_2 = \frac{1}{2} \int_0^\infty dz_1 \rho(z_1) \int_{\max(0, z_1 - d)}^\infty dr_{12} r_{12}^3 u'(r_{12}) \int_0^{\theta\,max} d\theta_{12} \sin\theta_{12} \rho(z_{12}) g^{(2)}(z_1, z_2, r_{12})$$

$$\times \int_0^{2\pi} d\phi_{12}(\sin^2\theta_{12}\cos^2\phi_{12} - \cos^2\theta_{12})$$

$$+ \frac{1}{2} \int_d^\infty dz_1 \rho(z_1) \int_0^{z_1 - d} dr_{12} r_{12}^3 u'(r_{12}) \rho(z_2) g_l(r_{12}) \int_0^\pi d\theta_{12} \sin\theta_{12} \int_0^{2\pi} d\phi_{12}(\sin^2\theta_{12}\cos^2\phi_{12} - \cos^2\theta_{12}), \quad \text{(A2)}$$

where $\cos\theta_{max} = \max(-z_1/r_{12}, -1)$.

Integrating over the solid angle of the second part vanishes, because both particles are in bulk liquid

phase, where the density $\rho(z)$ and $g^{(2)}$ function are independent of the solid angle.

Setting $\omega = \cos\theta_{12}$, and integrating the first term over ϕ_{12}

$$\gamma_2 = \frac{\pi}{2} \int_0^\infty dz_1 \rho(z_1) \int_{\max(0,z_1-d)}^\infty dr_{12} r_{12}^3 u'(r_{12}) \int_{\max(-1,-z_1/r_{12})}^1 d\omega(1-3\omega^2) \rho(z_2) g^{(2)}(z_1,z_2,r_{12}) \ . \tag{A3}$$

This is Eq. (4) in the text.

The integration over r_{12} depends on phenomenological functions, and cannot be carried out analytically. But the integration over z_1 and z_2 can be done explicitly. We therefore interchange r_{12} and z_1 and keep r_{12} as the last variable to be integrated. This leads to

$$\gamma_2 = \frac{\pi}{2} \int_0^\infty dr_{12} r_{12}^3 u'(r_{12}) \int_0^{r_{12}+d} dz_1 \rho(z_1) \int_{\max(-1,-z_1/r_{12})}^1 d\omega(1-3\omega^2) \rho(z_2) g^{(2)}(z_1,z_2,r_{12}) \ . \tag{A4}$$

Replacing ω by z_2,

$$\gamma_2 = \frac{\pi}{2} \int_0^\infty dr_{12} u'(r_{12}) \int_0^{r_{12}+d} dz_1 \rho(z_1) \int_{\max(0,z_1-r_{12})}^{z_1+r_{12}} dz_2 \rho(z_2)[r_{12}^2 - 3(z_1-z_2)^2] g^{(2)}(z_1,z_2,r_{12}) \ . \tag{A5}$$

This is Eq. (5), and the region of integration over z_1 and z_2 is given in Fig. 2 as the shaded area. Note that this region of integration is not symmetric with respect to z_1 and z_2. The calculation can be greatly simplified if we restore the symmetry. This can be done by subtracting from γ_2 the well-known expression γ_F of Eq. (6) written explicitly as

$$\gamma_F = \frac{\pi}{2} \int_0^\infty dr_{12} u'(r_{12}) \int_0^{r_{12}+d} dz_1 \rho_I \Theta(z_1/d) \int_{\max(0,z_1-r_{12})}^{z_1+r_{12}} dz_2 \rho_I \Theta(z_2/d)[r_{12}^2 - 3(z_1-z_2)^2] g^{(2)}(z_1,z_2,r_{12}) \ , \tag{A6}$$

where $\Theta(x)$ is the usual step function.

The region of integration of the difference $\Delta\gamma = \gamma_2 - \gamma_F$ now consists of two parallelograms symmetric with respect to $z_1 = z_2$ axis, i.e.,

$$\gamma_2 - \gamma_F = \frac{\pi}{2} \int_0^\infty dr_{12} u'(r_{12}) \left(\int_0^d dz_1 \int_{z_1}^{z_1+r_{12}} dz_2 + \int_0^d dz_2 \int_{z_2}^{z_2+r_{12}} dz_1 \right) I(z_1,z_2,r_{12}) \ , \tag{A7}$$

where

$$I(z_1,z_2,r_{12}) = \rho(z_1)\rho(z_2)[r_{12}^2 - 3(z_1-z_2)^2] g^{(2)}(z_1,z_2,r_{12}) \ .$$

Since $I(z_1,z_2,r_{12}) = I(z_2,z_1,r_{12})$, the two integration terms are identical and can be reduced to Eq. (7).

The rest of the algebraic procedures leading to the explicit expressions of Eq. (8a) to Eq. (8f) are straightforward. They are, however, much less tedious than the calculations based on the superficial density functions.

[1]R. D. Present and Chia C. Shih, J. Chem. Phys. **64**, 2262 (1976); R. D. Present, Chia C. Shih, and Yea H. Uang, Phys. Rev. A **14**, 863 (1976).

[2]J. G. Kirkwood and F. P. Buff, J. Chem. Phys. **17**, 338 (1949); F. P. Buff, Z. Elektrochem. **56**, 311 (1952).

[3]R. H. Fowler, Proc. R. Soc. A **159**, 229 (1937).

[4]S. Toxvaerd, J. Chem. Phys. **55**, 3116 (1971).

[5]J. L. Yarnell, M. J. Katz, R. G. Wentzel, and S. H. Koenig, Phys. Rev. A **7**, 2130 (1973).

[6]J. K. Lee, J. A. Barker, and G. M. Pound, J. Chem. Phys. **60**, 1976 (1974).

[7]J. A. Barker and D. Henderson, J. Chem. Phys. **47**, 4714 (1967).

[8]R. D. Present and C. T. Chen, J. Chem. Phys. **60**, 5133 (1974).

[9]J. A. Barker, R. A. Fisher, and R. O. Watts, Mol. Phys. **21**, 657 (1971).

[10]J. M. Parson, P. E. Siska, and Y. T. Lee, J. Chem.

Phys. **56**, 1511 (1972).

[11]J. Miyazaki, J. A. Barker, and G. M. Pound, J. Chem. Phys. **64**, 3364 (1976).

[12]G. A. Chapela, G. Savilla, and J. S. Rowlinson, Disc. Faraday Soc. **59**, 22 (1975).

[13]*Note added in proof.* The most recent Monte Carlo calculation by M. Rao and D. Levesque [J. Chem. Phys. **65**, 3233 (1976)] leads to $\gamma_2 = 12.2 \pm 0.43$ dyn/cm at 84 °K which is consistent to the results reported here.

[14]D. Fitts, Physica **42**, 205 (1969).

[15]K. S. C. Freeman and I. R. McDonald, Mol. Phys. **26**, 529 (1973).

[16]This is the simplest nontrivial phenomenological parametrization involving mixing of g_l and g_v, although it is ambiguous at $z_1 < d$, $z_2 = d$.

[17]P. A. Egelstaff and B. Widom, J. Chem. Phys. **53**, 2667 (1970).